Iranian Journal of Chemistry and Chemical Engineering (IJCCE)

Development of a Robust self-healing anticorrosion coating via one-pot electrochemically deposited SiO_2/linseed on carbon steel electrode

Reyhaneh Dehghanian[a], Parviz Aberoomand Azar[a,*], Ali Parsa[b], Mohammad Saber Tehrani[a], Susan Samadi[b]

[a]Department of Chemistry, Science and Research Branch, Islamic Azad University, Tehran, Iran

[b]Department of Chemistry, College of Science, Yadegar-e-Imam Khomeini (RAH) Shahre Rey Branch, Islamic Azad University, Tehran, Iran

Abstract

This work presents a novel self-healing/anti-corrosion coating based on epoxy resin decorated with electrochemically deposited silicon dioxide (SiO_2)/linseed oil (LO). For this purpose, the SiO_2/LO composite was prepared via a one-pot electrochemical deposition method, which was then utilized as a precursor for epoxy coating preparation. Various techniques, including Fourier transform infrared spectroscopy (FTIR), scanning electron microscopy (SEM), energy dispersive x-ray spectroscopy (EDS), thermogravimetric analysis (TGA), and X-ray diffraction analysis (XRD) were used to characterize the coated steel samples. Corrosion current and corrosion potential were decreased following the addition of SiO_2 and LO to the steel surface. The mechanism of improved anticorrosion performance of the composite coating can be attributed to the synergistic effect of the components within the composite film. The effect of various coatings on the anticorrosive characteristics of the self-healing coatings has been investigated by electrochemical impedance spectroscopy (EIS), Tafel plots, salt spray, and optical images. The defected self-healing coating consisting of epoxy/SiO_2/LO exhibited exceptional healing ability and corrosion inhibition performance toward steel metal as evidenced by EIS and optical images. The SiO_2/LO coating layer shows the lowest corrosion current of 0.091 $\mu A/cm^2$ compared to SiO_2 with 0.822 $\mu A/cm^2$ in corrosive saline media. Furthermore, epoxy coated SiO_2/linseed oil and epoxy coated SiO_2 films on steel supports exhibit corrosion resistances of 1.95×10^8 and 7.20×10^7 Ω/cm^2 demonstrating better performance of silica containing linseed oil. It seems that the addition of a hydrophobic linseed oil component can successfully delay the diffusion of water molecules or electrolyte ions, resulting in the improvement of anticorrosion characteristics of the coating layer.

Keywords*: Self-healing; Electrochemical deposition; Silicon dioxide; Linseed oil; Corrosion protection*

1. Introduction

Corrosion is a spontaneous ($\Delta G<0$) electrochemical procedure and is an expected manner of material degradation owing to exposure to corrosive media. Thus, it practically seems that stopping the corrosion procedure is impossible and instead of it could be tuned or retarded via appropriate methods. There are two modes of corrosion control methodologies named as either active or passive modes. Cathodic and anodic protection as well as utilization of corrosion inhibitors are examples of active modes, whereas passive routes mostly emphasize the material's type (alloys) and coatings (metal or non-metal) [1, 2]. Compared to the passive coating mode, the active mode still provides corrosion inhibition even while the coating is physically damaged. The most effective coating as an active coating for metals is chromate coating, and its widespread usage has been limited owing to its highly toxic benign [3-5]. Thus, finding a new alternative active material without a negative environmental impact is of great importance [6-9]. Research in the field of environmentally friendly corrosion inhibitors and the use of cheap and effective compounds with low environmental impacts has been carried out extensively [10,11].

One of the most practical methods to protect metals against corrosion is the use of organic molecules, which has become more popular [12,13]. The most common route for shielding the steel surface from corrosion is the use of organic coatings like epoxy coatings that cannot deliver long-term protection and their performance normally deteriorates during exposure to corrosive media [5, 14]. To address this issue, self-healing coatings, have received increasing emphasis in recent decades [15-18]. Motivated by nature, self-healing coating materials have gained tremendous consideration owing to the large lifespan and ease of application of these protective materials [19-21]. In fact, the self-healing coatings could deliver healing materials to the metal substrate to impede corrosion expansion while the main coating material is damaged following exposure to corrosive circumstances [22]. A self-healing agent has been embedded through the coating, and it releases whenever is needed [23,24]. When a crack is created through a coating, the self-healing agent is released from the coating and the crack has been repaired following the release of this component [25,26]. However, several kinds of materials have been utilized as healing reagents in combination with epoxy resins like dicyclopentadiene (DCPD) [27], phenylacetate (PA), chlorobenzene (CB), linseed oil [28,29], tung oil (TO) [30], perfluorooctyl triethoxy-silane (POT) [31], isophorone diisocyanate (IPDI) [32], and so on. Among these materials, LO as a healing reagent has a large amount of unsaturated fatty acids with eco-friendly properties and high thermal stability [22]. The first report on the utilization of LO to make the epoxy based self-healing coating was presented by Suryanarayana et al. [33]. Since then, research papers that use LO as a self-healing material have been growing [34, 35]. Owing to the free radical oxidation of unsaturated double bands present in the composition of LO by oxygen, LO is recognized as one of the most important oils for self-healing aims in the coatings. The formation of bonds between the LO's molecules produces a solid layer that gives the surface water repellency characteristics and makes the surface impermeable to many chemical reagents [36]. Therefore, the LO coating performance fails in the corrosive media due to the formation of conductive pathways within the coating [35]. However, the usage of these coatings in combination with other anticorrosive reagents could be the solution method for the development of new coating layers with superior performance as compared to single-component coatings.

Among the various micro- and nanomaterials utilized as co-coating layers for self-healing coatings, silicon dioxide (SiO_2) nanomaterials have marvelous characteristics that encourage researchers to discover and develop new hybrid coatings by the presence of SiO_2. This nanomaterial based self-healing coatings could possess some

advantages such as uniform distribution of the healing agent through the coatings, high loading of healing agent owing to large surface areas and pore volumes, high mechanical and physical durability, and entrapment of large amounts of air to form an air layer at the interfacial area of solid-liquid which could be helpful, especially for anticorrosion coatings [36]. Several methods have been developed for the formation of such coatings, including sol-gel [37], electro-spinning [38], electrodeposition [39], etc. Among these routes, electrodeposition has drowned immense consideration owing to high accuracy, simplicity, cost-effectiveness as well as simple equipment and possible simple manipulation [39,40]. Up to now, several attempts have been made for electrodeposition of SiO_2 hybrid coatings. In this case, Wu and Collagenous fabricated the SiO_2 coating film by sol-gel electrochemical deposition and viewed that the SiO_2 coating showed good water repellency, high chemical and physical stability, and great mechanical properties [41]. In other research, Liu and co-workers electrochemically deposited the porous film of SiO_2 on the surface of mild steel. Then, it was utilized as support for the loading of various corrosion inhibitors consisting of polyvinylpyrrolidone (PVP) and zinc gluconate. Moreover, the pre-processed mild steel was painted using epoxy resin and the final coating showed superior corrosion resistance performance as compared to single-component coatings [6]. The same group has reported superhydrophobic coating on a mild steel substrate with the assistance of an electrodeposition strategy [42].

There are several reports of the use of LO as a healing agent [43, 44]. Szabó et al. synthesized core–shell microcapsules composed of urea-resorcinol-formaldehyde (UF) and LO as shell and core materials, respectively, as paint additives for self-healing coatings. The coating material consisting of core-shell self-healing octadecylamine (ODA) and Co-octoate, revealed the best anticorrosion performance [44]. Hasanzadeh et al. prepared microcapsules of UF as the shell and LO as the healing material which can be loaded by CeO_2 nanoparticles (NPs) and finally used as a coating material for carbon steel metal [34]. Zhou et al. reported a triple-function smart anticorrosion composite coating based on graphene and ZIF-8 with excellent pH-responsive self-healing [45]. Ren et al. developed a self-healing epoxy composite coating based on pH-responsive PCN-222 smart containers for long-term anticorrosion of aluminum alloy [46]. However, synthesis procedures utilized for the preparation of hybrid coatings containing both SiO_2 and LO have advantages and disadvantages. Most of these methods suffer from labor and time-consuming procedures and thus searching for discovering a one-step, simple, fast, and scalable strategy is of great importance.

The authors propose a novel self-healing/anti-corrosion coating based on epoxy resin decorated with electrochemically deposited silicon dioxide (SiO_2) and linseed oil (LO). The combination of SiO_2 and LO in the coating provides synergistic effects, contributing to improved anticorrosion performance. SiO_2 nanoparticles offer advantages such as uniform distribution of the healing agent, high loading capacity, and mechanical durability. Linseed oil, known for its eco-friendly properties and high thermal stability, acts as a healing reagent. The novelty of this work lies in the one-pot electrochemical deposition method used to prepare the SiO_2/LO composite, which serves as a precursor for the epoxy coating. This method offers simplicity, cost-effectiveness, and scalability compared to other synthesis procedures. The authors highlight that the use of this innovative strategy can lead to the development of robust self-healing anticorrosion coatings with superior performance compared to single-component coatings. The evaluation of the coating's performance was performed through various characterization techniques and corrosion testing methods.

2. Experimental

2.1. Materials

The steel panels were prepared from the local market. Before use, steel panels with a thickness of 0.1 cm were cut into 2.0 cm×1.0 cm pieces followed by abrasion with emery papers of various grades 400, 600 and 1200. Ethanol (EtOH) (≥ 96 % v/v), acetone (99 % v/v), and tetraethoxysilane (TEOS, >99 %) were purchased from Merck company (Darmstadt, Germany). All other chemicals were bought from Sigma-Aldrich and were of analytical grade and used as received without any further purification.

2.2. Apparatus

Electrochemical studies were performed via an Ivium CompactStat (Netherlands). The functional groups of the coated steel panels were determined via an ATR-FTIR spectrometer (Bruker Optics GmbH, Ettlingen, Germany) in the frequency range of 600-4000 cm^{-1}. The surface morphology of bare steel and coated steel plates was studied by FE-SEM (FE-SEM, Mira 3-XMU) equipped with an EDS detector (LEO 9121413). Phase characterization was investigated by XRD via the X'Pert PANalytical X-ray diffractometer (Netherlands) with a Cu anode (λCuKα=1.54 Å) as the radiation source. The thermal stability of SiO_2 and SiO_2/LO species was assessed by TGA (STA 1500) at a heating speed of 10 °C/min under N_2 gas flow. An optical microscope (JM300) has been used for the observation of scratched steel panels.

2.3. Electrochemical deposition of SiO_2 and SiO_2/LO coatings on steel panels

The pretreated steel specimens were utilized as substrates for the electrochemical deposition of SiO_2 and SiO_2/LO coatings in a one-pot sol-gel electrochemical deposition procedure. For this purpose, a three electrode configuration has been utilized by using steel plates, Pt plate and Ag/AgCl (KCl saturated) as working, auxiliary, and reference electrodes, respectively. A single step amperometric plateau by using a constant cathodic potential of -1.3 V was applied for electrodeposition of SiO_2 and SiO_2 containing healing agent. In a typical synthesis procedure, an electrodeposition bath was containing of 5 mL TEOS, 50 mL EtOH, and 50 mL aqueous solution of $NaNO_3$ (0.2 M). The pH of the solution was adjusted by the addition of adequate amounts of HNO_3 or NaOH (pH≈3). Before electrodeposition, the precursor solution was agitated under an ultrasonic bath at a fixed temperature of 25 ˚C for 2h. The electrochemical deposition step was performed for a time duration of 5 min. For the synthesis of SiO_2 containing LO (healing agent), a similar strategy was utilized rather than 0.5 mL of LO was added to the electrodeposition bath media. After that, the as-prepared coated samples were dried in an oven at 60 ˚C for 2 h. It must also be emphasized that the exposed surface area of steel samples to the solution was about 1 cm^2.

2.4. Epoxy resin coated steel samples

The epoxy resin coated steel panels were prepared in similar conditions reported by Liu and coworkers with some modifications [15]. Epoxy resin and polyamide resin (5/4 mass ratios) were mixed with xylene and n-butanol solvents with a volume fraction of 7:3. The mixture was treated sonically for 1 h, and then the steel plates were coated with epoxy resin using a brush. The coated steels were kept at r.t for about 2 h, and then it was cured at 60 ˚C for 48 h and after that, it was stored for 1 day before electrochemical tests. For evaluation of the performance of various coatings, different coating arrangements were fabricated: epoxy layer onto the pure steel panel (E/SS),

epoxy layer coated onto electrodeposited SiO_2 onto the steel panel (E/ SiO_2/SS) and epoxy layer coated onto electrodeposited SiO_2-LO onto the steel panel (E/SiO_2-LO/SS).

2.5. Electrochemical measurements

Electrochemical measurements consisting of Tafel and EIS tests were conducted to evaluate the anticorrosion properties as well as the self-healing capability of the prepared coatings. For self-healing investigations, the coating steel panels were scratched and immediately immersed in 3.5 wt% NaCl solution as corrosive media. Electrochemical impedance spectroscopy tests were done at an open circuit potential by applying a sinusoidal perturbation potential of as high as 10 mV over the frequency range of 100 kHz to 10 MHz. The goodness of model fitting was estimated by the parameter known as Chi-squared (χ^2). The smaller the χ^2, the better the model fitting (Chi-squared$\leq$ 0.001). However, this is not the only criterion for the best model fitting. The equivalent circuit elements must address the possible physical procedure at the electrode/electrolyte interfacial area. In all cases, the chi-squared quantities were lower than 0.001 demonstrating good model fitting and the suitability of elements selected for model fitting [47]. All electrochemical studies were carried out in a three-electrode configuration, whereas the coated steels (1cm×1cm), Ag/AgCl and Pt plate (1cm×2cm) were used as working, reference, and the auxiliary electrodes, respectively. For all measurements, the exposed area of the working electrode in connection with the electrolyte was about 1 cm^2. The potentiodynamic polarization plots (Tafel) were recorded from negative potentials to positive ones with a potential scan rate of 0.5 mV/s. Before measurements, all samples were submerged in 3.5 wt% NaCl aqueous solution for 10 min for the establishment of equilibrium between the samples and corrosive media.

2.6 Salt spray test

The visual corrosion resistance of self-healing coatings on steel supports was evaluated using the ASTM B117 salt spray method. The edge and backside of the steel substrates were covered with water-resistant glue. After that, the coated steels were placed in a salt spray chamber containing 5 % NaCl as fogging medium. The salt spray chamber temperature was tuned to 35±2 °C. Then, the coated samples were scratched and inserted in the salt spray chamber for 96 h.

3. Result and discussions

3.1. Coating materials

The facile and scalable one-pot sol-gel electrochemical deposition strategy has been applied for electrodeposition of SiO_2 and SiO_2 containing LO coatings onto the surface of steel plates. The idea of sol-gel electrochemistry comes from the fact that applying negative potential could accelerate the condensation interactions of silane containing moieties. By applying the negative potential to the cathode electrode (steel electrode in this case), the pH of the electrode increases owing to water/oxygen reduction or in some cases electrolyte reactions (e.g. nitrate ions). Each of the above-mentioned reactions could induce the production of hydroxyl ions, which further increases the condensation reaction rate of the sol near the cathode surface and provides additional motivating force for the deposition of SiO_2 structures onto the surface of the cathode electrode [41]. Scheme 1 shows the

detail of the electrochemical strategy applied for the precipitation of porous SiO_2 based film coatings onto the surface of the steel substrate along with its anticorrosion performance against corrosive media.

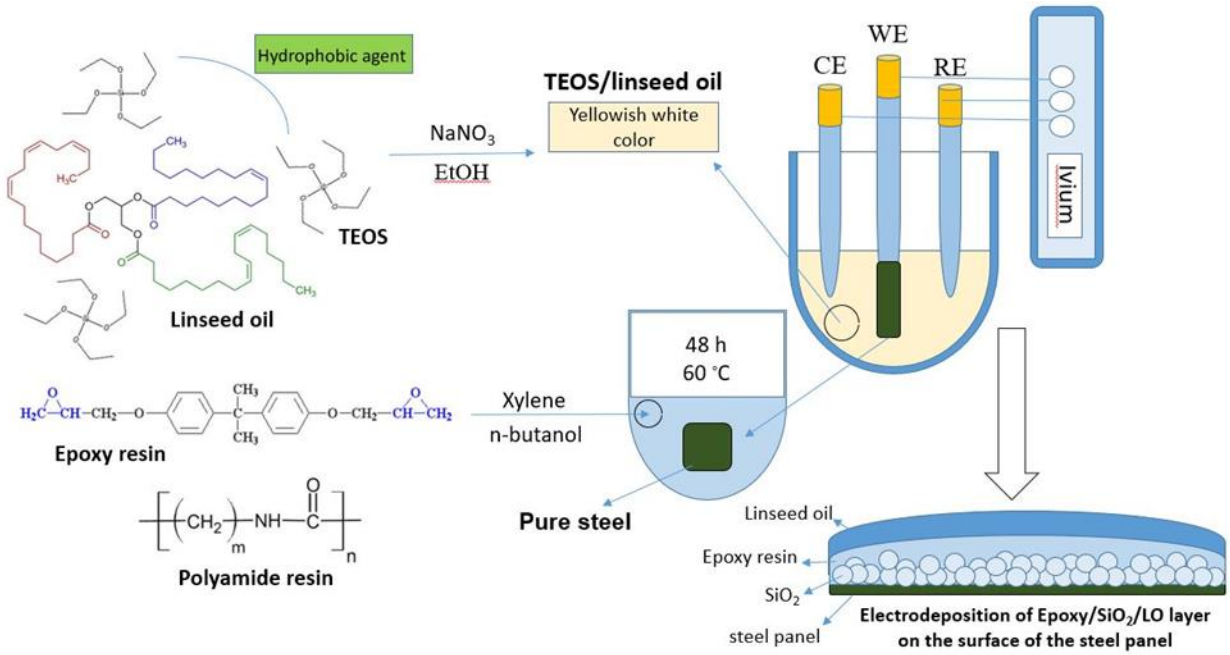

Scheme 1. Schematic illustration of electrodeposition of SiO_2 microstructures containing LO on the surface of the steel panel and its anticorrosive performance against corrosive media.

3.2. Characterization

3.2.1. FTIR analysis

Fig 1 exhibits the IR spectra of the electrochemically deposited SiO_2 based coatings onto the steel substrate. For electrodeposited SiO_2, sharp absorption bands at about 1050 and 794 cm^{-1} are related to the asymmetric and symmetric stretching modes of Si-O-Si bonds, respectively. An observed shoulder at about 958 cm^{-1} corresponds to the stretching mode of the Si–OH bond [48,49]. For the FTIR spectrum of the coating material containing LO, the bands at around 2922 and 2852 cm^{-1} are ascribed to the stretching vibrations of C−H related to the $-CH_2-$ and $-CH_3$ groups. The peak at 1737 cm^{-1} is related to the stretching vibration of the carbonyl group present as the COOH functional group. The stretching vibration of $-CH_3$ is represented at 1458 cm^{-1}. The characteristic peak at about 718 cm^{-1} is assigned to the bending vibration of the unsaturated =C−H bond, whereas its corresponding stretching vibration band is overlapped via the broad stretching vibrational peak of the OH functional group [50]. However, the shift in the band positions of SiO_2 containing LO as compared to pure SiO_2 coating reveals that the O–Si–O network is influenced by the existence of LO in its surrounding area.

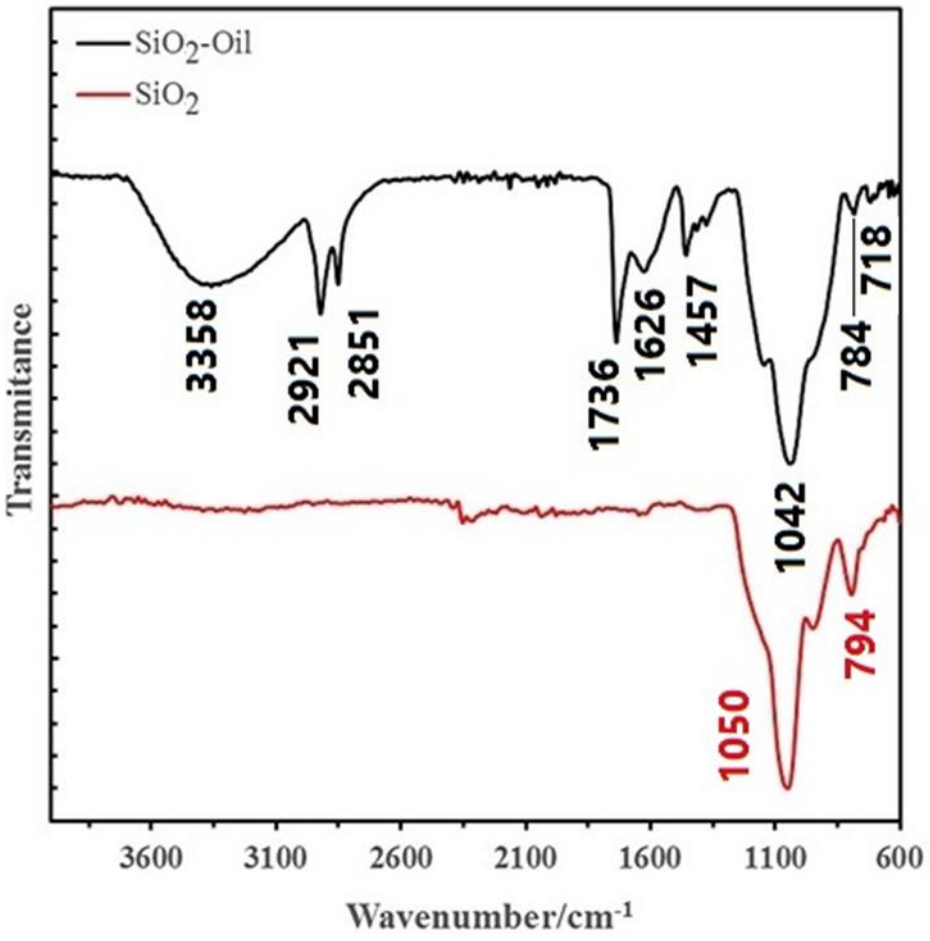

Figure 1. ATR-FTIR spectra of coated steel panels after electrodeposition step

3.2.2. SEM analysis

Mechanical treatment of steel plates with sandpaper and then washing them resulted in the formation of a nearly rough surface (Fig. 2A). In the case of electrochemically deposited SiO_2 coating onto the steel substrate, the highly rough layer containing many grooves was detected. This may come from the releasing of gaseous hydrogen following water reduction at the near surface of the cathode electrode (Fig. 2B). Higher magnified SEM image revealed that precipitated silica structures have spherical morphology with the dimensions of about 61-99 nm (Fig. 2B and 2C). After the introduction of LO to the electrodeposition bath, the surface morphology of the deposited film was undoubtedly changed, which means that LO could affect the electrodeposition of SiO_2 film onto steel support. Additionally, the interfacial area among the spherical silica particles was filled by the LO and the deposited film became more compact and the roughness of the coating layer was decreased following the usage of LO in the electrodeposition bath media (Fig. 2D, 2E, and 2F). However, it seems that the introduction of LO does not change the electrodeposition mechanism of SiO_2 microspheres, since the overall microstructure morphology of SiO_2 coating film remains unchanged.

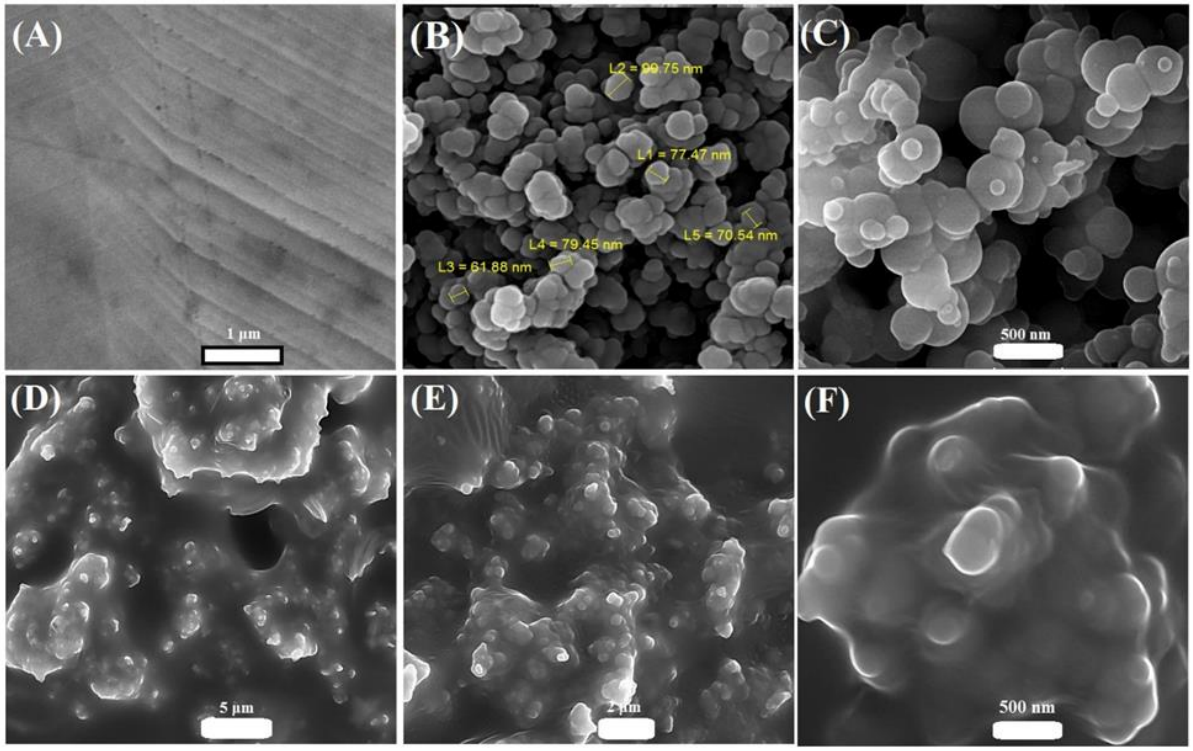

Figure 2. SEM images of (A) pre-treated steel plate, (B and C) steel coated SiO_2 at various magnifications, and (D, E and F) steel coated SiO_2/LO at various magnifications

3.2.3. EDS analysis

The EDS spectra along with elemental analysis of the steel panel were monitored, and results are presented in Fig 3. EDS spectrum displays the weight percentages of Fe (73.29%), Cr (18.68%), Ni (7.56%), Si (0.34%), and Al (0.12%), which confirmed the presence of steel substrate.

The EDS analysis and elemental mapping analysis of coated steel samples are exhibited in Fig. 4 and Fig. 5. EDS mappings of SiO_2 coated steel plate demonstrated the homogenous distribution of C, O, and Si elements in its structure. This observation undoubtedly proves the successful precipitation of the SiO_2 layer onto the surface of the steel substrate. In addition, the presence of Fe (49.05%), Cr (13.19%), and Ni (4.63%) elements in the EDS spectra is related to the steel substrate (Fig. 4). In the SiO_2/LO coating (Fig. 5), it can be observed that the percentage of C element is increased as compared with SiO_2 coating layer, which indicated the successful loading of LO into the layer. Furthermore, the quantitative elemental analysis by EDS spectra reveals that the percentage of elements corresponding to steel substrate was significantly decreased in the composite coating, which revealed the denser and thicker benign of the composite coating layer. The EDS elemental maps of the SiO_2/LO coating proved the high uniformity and high carbon content of the coating on the surface of the steel substrate.

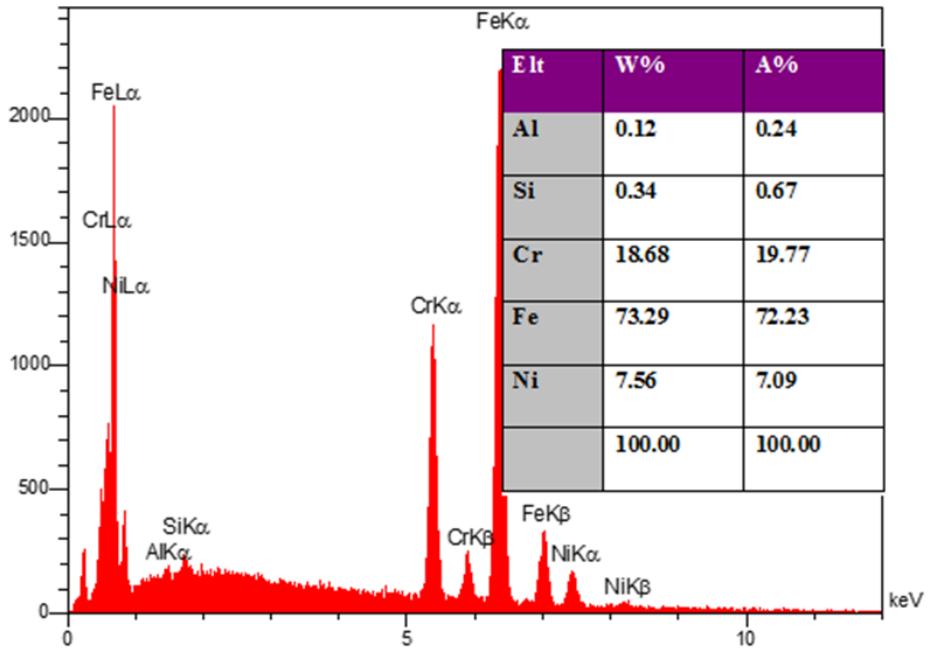

Elt	W%	A%
Al	0.12	0.24
Si	0.34	0.67
Cr	18.68	19.77
Fe	73.29	72.23
Ni	7.56	7.09
	100.00	100.00

Figure 3. EDS spectra and elemental analysis of steel substrate

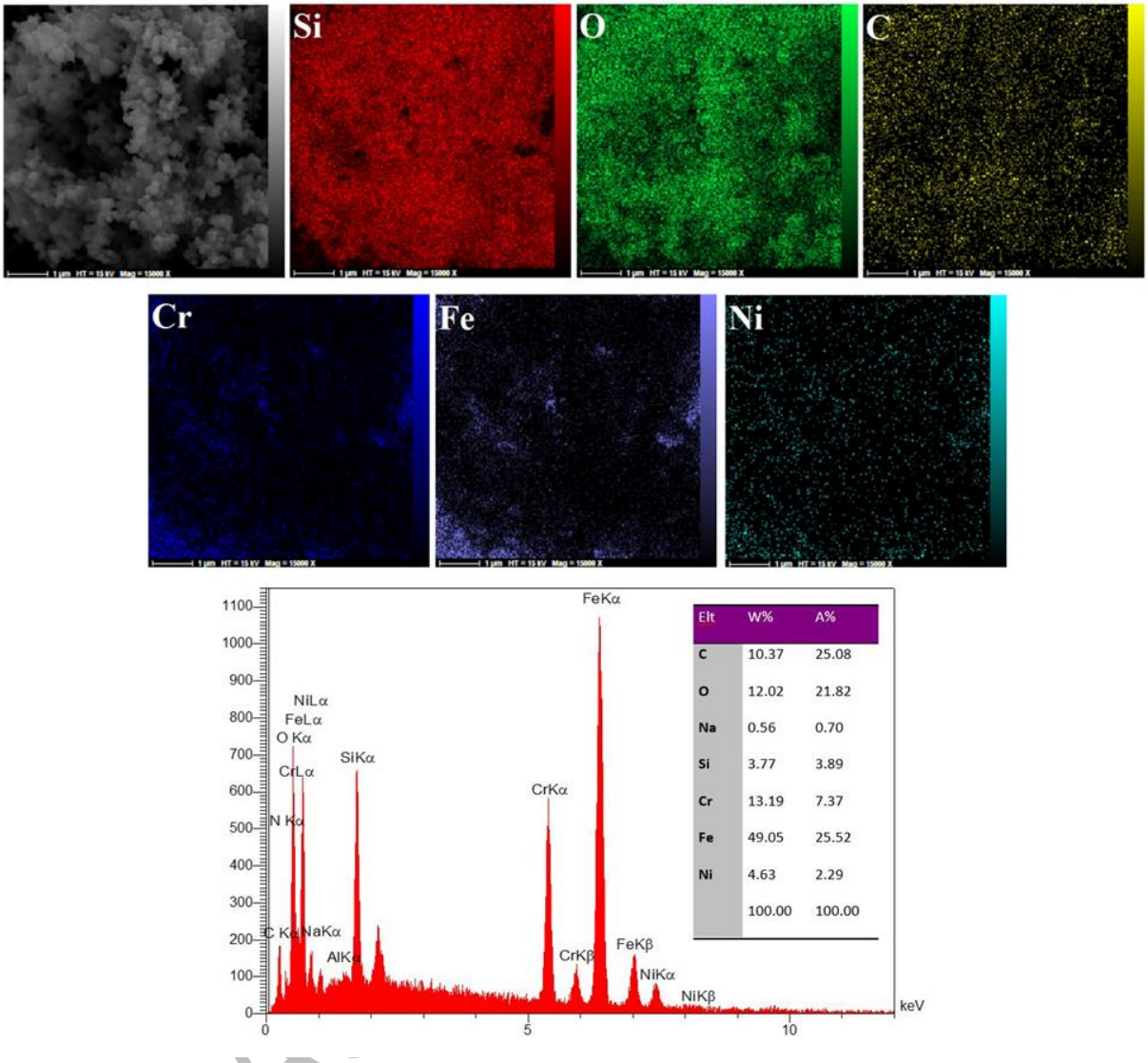

Figure 4. SEM/EDS elemental analysis and EDS data of steel coated SiO_2 film

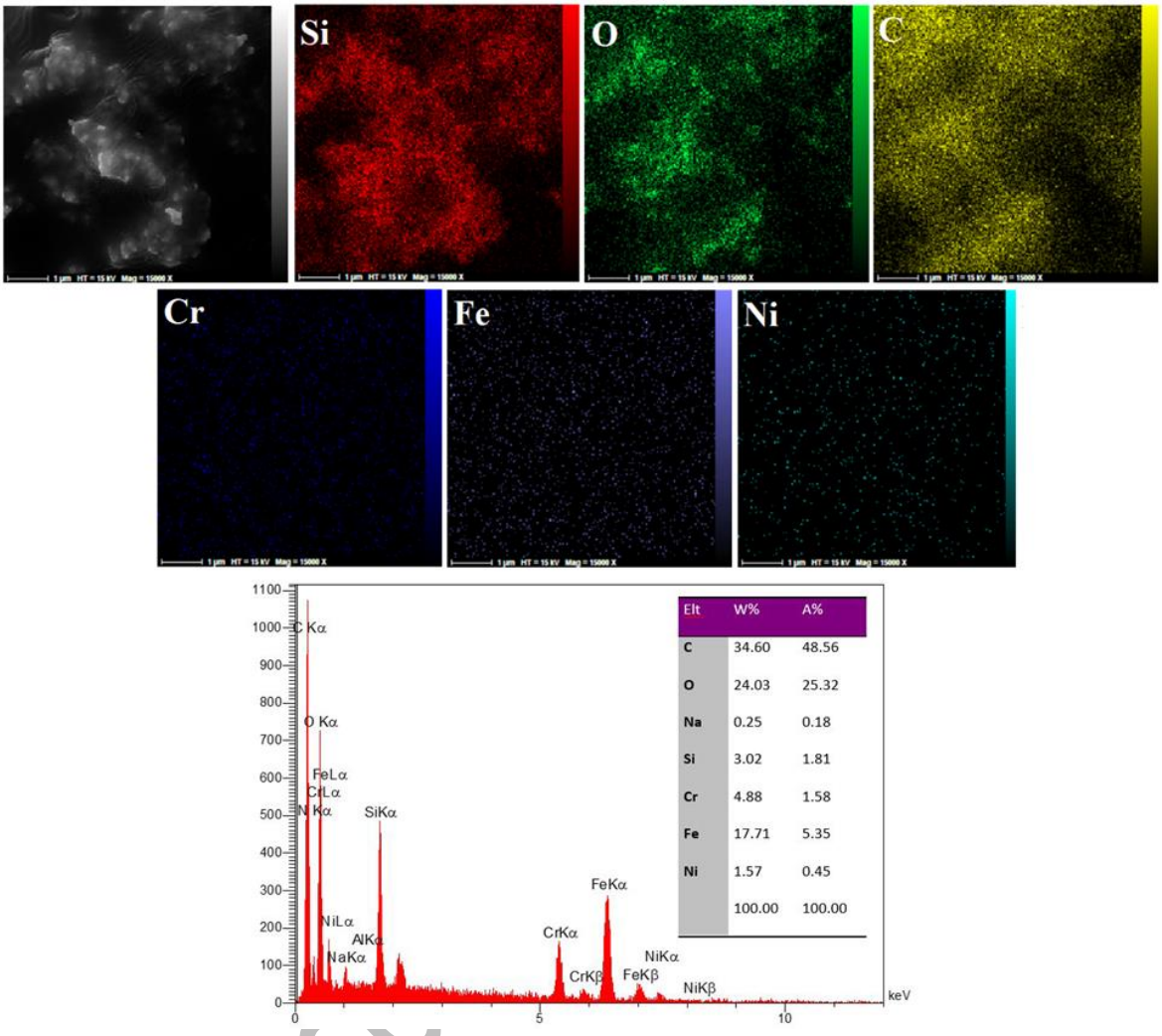

Figure 5. SEM/EDS elemental analysis and EDS spectra of steel coated SiO_2 film containing LO

3.2.4. TGA analysis

The thermal stability of SiO_2 and SiO_2/LO was assessed by TGA analysis (Fig. 6). The samples were heated from room temperature to 800 °C at a heating speed of 10 °C.min^{-1} under N_2 gas flow. As it is obvious from TGA analysis, the SiO_2 material shows a weight loss at about 100 °C corresponding to loss of interfacial-adsorbed water molecules in the SiO_2 sample and after that, it preserves its stability until 800 ˚C under an inert nitrogen atmosphere. Thus, in the case of SiO_2/LO rather than a weight loss relating to adsorbed water molecules, a sharp weight loss in the range of 330-450 °C is attributed to the thermal decomposition of LO constituent within the composition of the composite coating. The difference in weight loss between the two samples could be used to calculate the loading of LO material in the composite material, which was about 41.6 %. The high loading of LO within the chemical profile of the composite coating could help improve the anticorrosion/self-healing performance of steel coated panels.

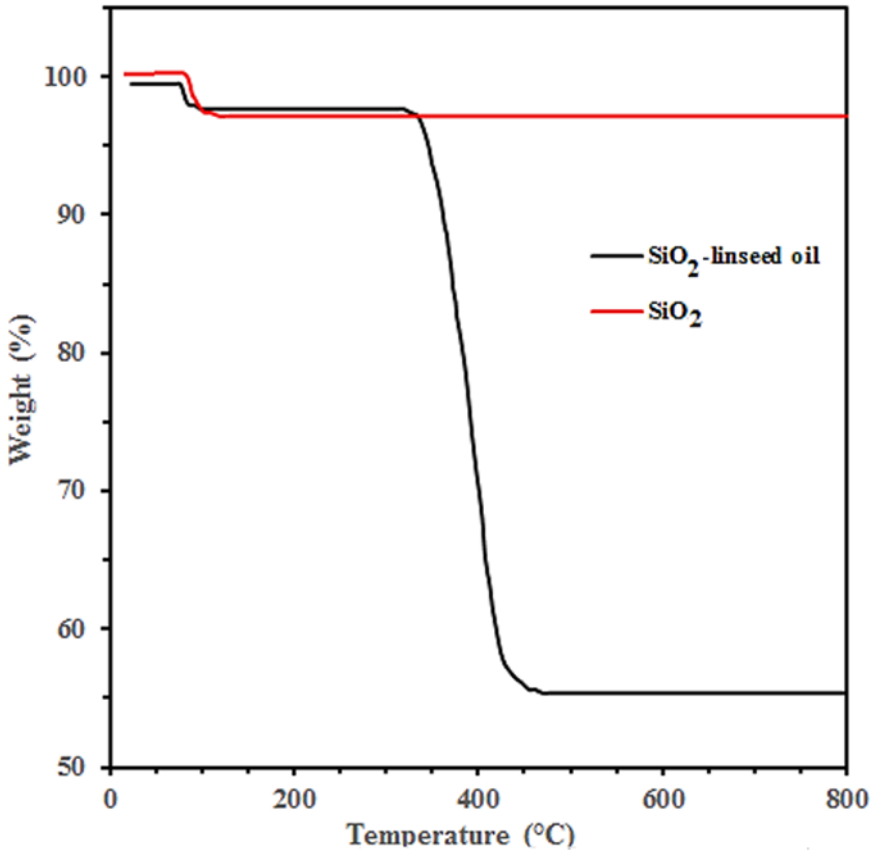

Figure 6. TGA profiles of the scratched electrodeposited SiO_2 and SiO_2/LO samples

3.2.5. XRD analysis

X-ray diffraction patterns of the as-prepared SiO_2 and SiO_2-LO coating films are shown in Fig 7. The prepared films are mainly composed of SiO_2 and the crystallographic results demonstrate that the major phase is crystalline SiO_2 at 2θ equal to 14.32° and 17.15°. It is also noteworthy that after the inclusion of LO within the coating film, the intensity of diffraction peaks was decreased demonstrating decreasing the crystallinity of the SiO2 because of the inclusion of amorphous linseed oil within the coating film.

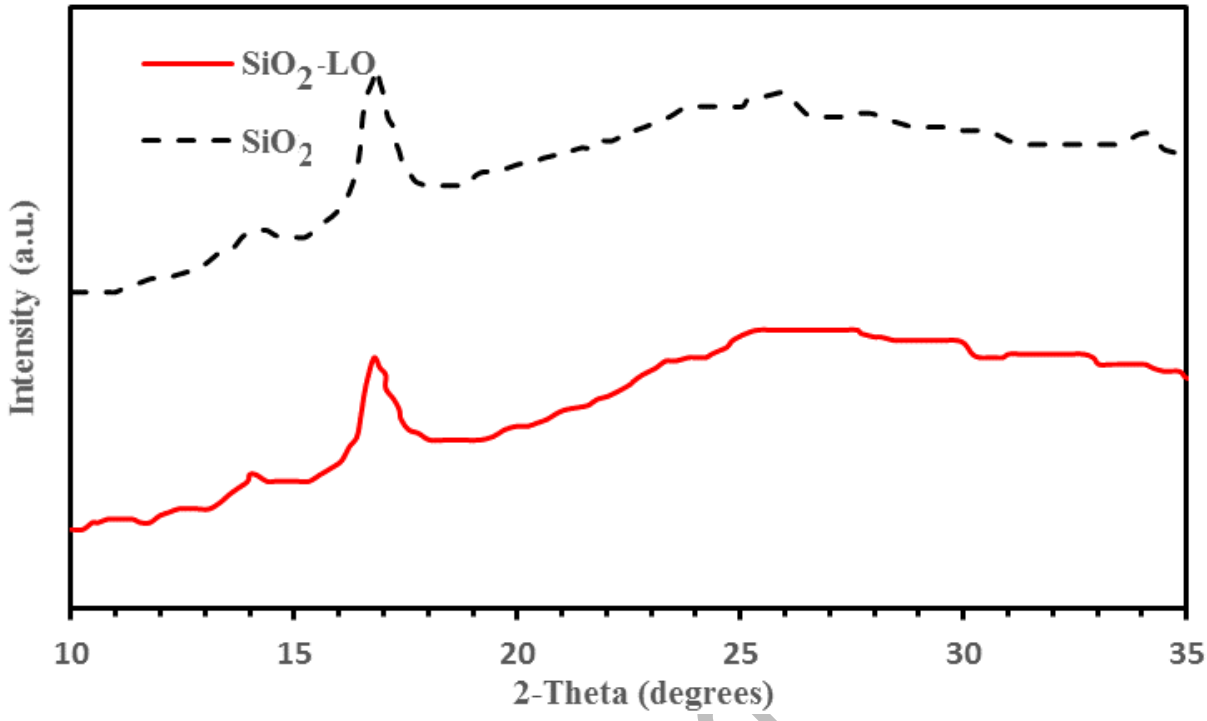

Figure 7. XRD patterns of steel coatind with SiO_2 (dashed black line) and SiO_2-linseed oil (solid red line)

3.3. Anticorrosion and self-healing characteristics of coatings

3.3.1. Anticorrosion investigation by Nyquist plots

The steel plates with various coating materials with an exposed area of 1 cm^2 were submerged in 3.5 %wt. saline solution and their anticorrosion performance were studied via EIS measurements as well as linear polarization experiments. To show the effect of LO on the corrosion resistance of steel panels, Nyquist plots of coated steel plates before epoxy coating in 3.5 wt% saline solution are illustrated in Fig 8. In each case, a depressed semicircle related to the charge transfer resistance was observed. The best fitted model was a model consisting of electrolyte resistance (R_s), charge transfer resistance (R_{ct}), and (constant phase element) (CPE) (inset of Fig 8). The CPE component has been utilized to show the non-ideality of the formed capacitance at the interfacial area of the electrolyte/electrode. R_s and R_{ct} elements are related to the solution resistance as well as the charge transfer resistance, respectively. The R_s value relates to the summation of the ohmic resistances within the electrochemical cell consisting of uncompensated solution resistance, contact resistance, and internal resistance of electrode material. The steel coated plates showed higher charge transfer resistances as compared to bare steel substrate owing to the protective benign of silica and LO components within the composition of the coating layer. Thus, the coated steel panel containing LO displayed the highest charge transfer resistance. These observations demonstrate that the addition of LO further retarding the availability of corrosive components in saline solution or from dissolved oxygen to the metal substrate surface. However, R_{ct} values were found to be 1104, 2001, and 3106 $\Omega.cm^2$ for bare stainless steel, SiO_2/SS, and SiO_2-LO/SS electrodes, respectively. The reason for the improvement of anticorrosion performance of silica coated steel in comparison to a bare steel plate is related to the fact that the electrochemically deposited film of SiO_2 can be attached firmly to the metallic supports owing to

the formation of the chemical binding between metal and SiO_2 by the assistance of OH^- ions following the applying a negative potential to the cathode electrode [42].

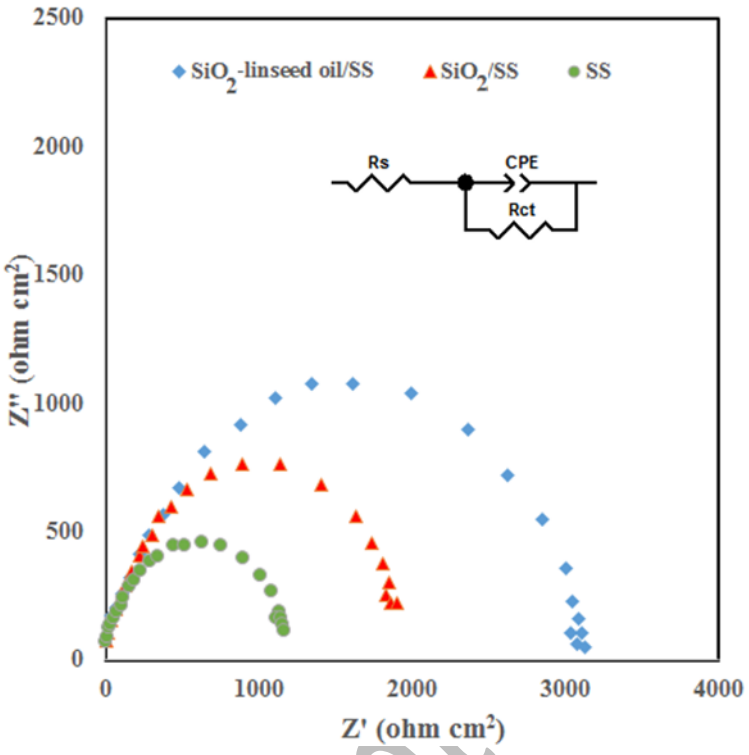

Figure 8. Nyquist plots of various prepared samples in 3.5 wt% NaCl solution

3.3.2. Self-healing investigation by Tafel plots

Polarization plots and related fitted parameters of the bare steel and coated steel samples are given in Fig 9 and Table 1. In this table, E_{corr}, I_{corr}, b_c, and b_a stand for the corrosion potential, corrosion current density, and the slope of the cathodic and anodic half-cycles, respectively. It is obvious that the corrosive potentials shift in the positive direction owing to decreasing the anodic dissolution of steel substrate following the addition of anticorrosive reagents. The coated sample consisting of silica microspheres and LO exhibits the highest anodic potential shift. The i_{corr} value of the steel panel was 4.3 µA/cm, which was decreased to 0.822 µA/cm for SS/SiO_2 and 0.091 µA/cm^2 for SS/SiO_2-LO. The lower the i_{corr}, the higher the corrosion resistance. From Table 1, it could be undoubtedly inferred that the electrodeposition of silica structures on the surface of the steel plate increased the corrosion resistance of the steel as compared to the bare steel panel. By contrast, the addition of LO to the electrodeposition media further increased the corrosion resistance against saline corrosive media. Therefore, it can be deduced that the coated samples show higher resistance against corrosive media by hindering the active sites of the steel panel. Moreover, the presence of LO would make the coating less rough and more compact, which ensuing the increasing of the corrosion resistance. The silica film not only enhances the diffusive pathway of corrosive ingredients to the surface of steel support but also enhances the corrosion potential of steel as evidenced by E_{corr} values. The increasing of the anodic and cathodic slope branches of coating steel panels as compared to blank steel sample one was related to the decreasing of anodic and cathodic reaction rates, respectively, revealing the mix of anodic/cathodic inhibition of the coating materials. The higher the Tafel slope

in mV/dec unit means that higher potentials should be applied for attaining a special current density. Moreover, the inhibition yield of various coatings was evaluated based on the following equation:

$$(\%\eta) = 100 \times (1-i'_{corr}/i_{corr}) \quad (1)$$

where η is the corrosion inhibition yield; i_{corr} and i'_{corr} are related to the corrosion current density in the absence and presence of coating materials, correspondingly. Corrosion inhibition yields for coated steel plates were found to be about 80.9% and 97.9% for SiO_2/SS and SiO_2/LO/SS, respectively. These findings further demonstrate the protective effects of the coatings on the steel panels.

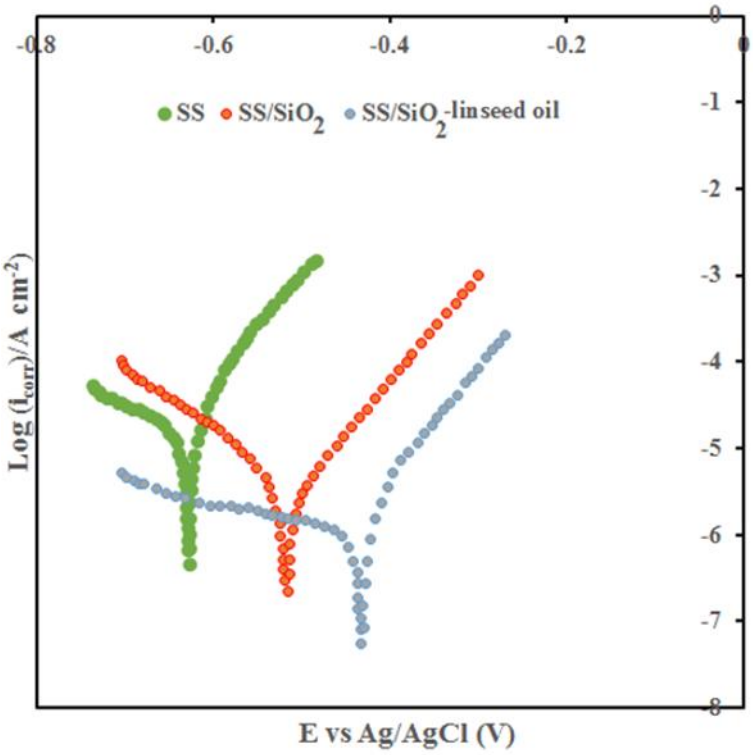

Figure 9. Tafel polarization plots of various coated stainless steel panels at scan rate of 0.5 mV/s

Table 1. Polarization parameters of bare steel and steel coated samples in saline media

System	E_{corr}/vs. Ag/AgCl (KCl_{sat}) (mV)	i_{corr} (μA/cm^2)	$-b_c$ (mV/dec)	b_a (mV/dec)
SS[a]	-694	4.3	26	43
SS/SiO_2	-565	0.822	51	54
SS/SiO_2-LO	-473	0.091	41	48

[a] Stainless steel

3.3.3. EIS measurements on the intact and scratched steel coated samples

3.3.3.1. Investigation impedance quantities of Non-defected coated

After complete characterization of the various electrodeposited coatings, the effect of epoxy resin incorporation into various electrodeposited formulation coatings containing SiO_2 microspheres and SiO_2 structures/LO on the corrosion resistance was assessed by EIS measurements on the intact and scratched steel coated samples (Fig 10). The impedance response of intact samples at the early stages of immersion in saline media was dominated by the capacitive behavior as shown by CPE rather than C_{dl} to denote the non-ideal capacitive characteristics of the coatings. However, there is a pure resistance behavior in the low-frequency domain, which is related to the resistance of the coating against charge propagation. The equivalent circuit related to the Bode curves has been shown in Fig. 9C. It was observed that the epoxy coated steel panel containing both LO and silica particles delivers the highest impedance quantities over the entire frequency range (Fig 10A, B). Table 2 denotes the electrochemical parameters attained from EIS data at the time of 0.5 h in 3.5 % NaCl. As shown in this Table, the obvious increase in R_{coat} quantity of epoxy coating in samples containing electrodeposited SiO_2 (3.64 times) and SiO_2-LO (4.56 times) demonstrated the extremely poor corrosion protection characteristics of the neat epoxy coating (E/SS) as compared with E-SiO_2/SS and E-SiO_2-LO/SS coated plates. Also, CPE_{coat} as a criterion was utilized for the estimation of the distribution of ionic species at the interfacial area between the coating and the electrolyte. The higher value of CPE_{coat} means that the coating is more potent to corrosion [51]. Thus, both R_{coat} and CPE_{coat} values showed that the epoxy coating containing both LO and silica microspheres has higher anticorrosion properties against corrosive media when compared to neat epoxy coating and an epoxy coating containing silica microspheres. The impedance values in the lowest frequency ($|Z|_{10\ mHz}$) were applied to visualize the variations of corrosion resistance. However, the ($|Z|_{10\ mHz}$) quantities of E-SiO_2-LO/SS, E-SiO_2/SS, and E/SS were found to be about 1.95×10^8, 7.2×10^7, and 1.87×10^7 $\Omega\ cm^2$, respectively. The larger impedance at the low-frequency region demonstrates the higher anticorrosive characteristics of the sample. Hence, the E-SiO_2-LO/SS shows the highest anticorrosive behavior, followed by E-SiO_2/SS and E/SS samples. The incorporation of various anticorrosion coatings significantly improved the coating barrier properties of the organic coating as compared to the pure coated epoxy steel sample. The chemical interaction among silica microparticles/LO and functionalities on the epoxy matrix may be responsible for the improvement of barrier characteristics and ionic resistance. More interestingly, silica microspheres can increase the contact area between the substrate and the epoxy coating film, which could help improve the barrier characteristics of the composite coating as compared to the pure epoxy coating sample.

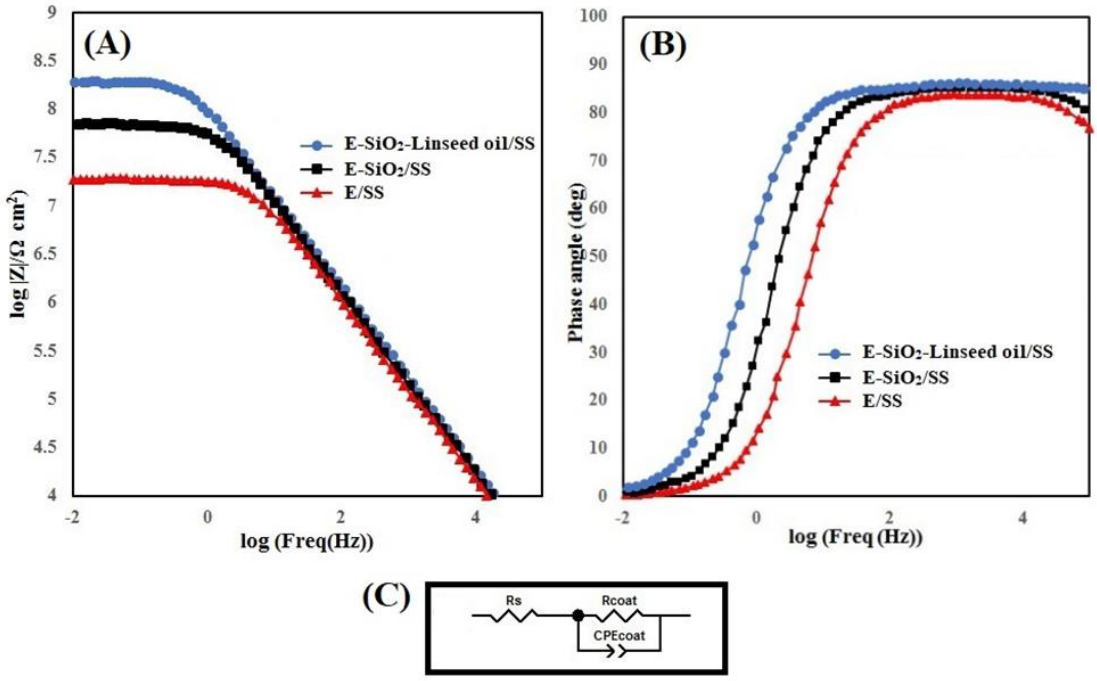

Figure 10. Typical Bode (A) and phase angle (B) plots of pure epoxy (E/SS), E-SiO₂/SS, and E-SiO₂-LO/SS after immersion in 3.5 wt% NaCl solution for 0.5 h, (C) Electrical equivalent circuit utilized for modeling of impedance spectra

Table 2. The electrochemical parameters of various steel coated samples containing E/SS, E-SiO₂/SS, and E-SiO₂-LO/SS after immersion in 3.5 wt% NaCl solution for 0.5 h

Electrode	CPE_{coat}		R_{coat} (Ω cm^2)
	Y_0 (Ω^{-1} $cm^{-2}S^n$)	n_{coat}	
E[a]/SS	2.3×10^{-9}	0.9	1.87×10^{7}
E-SiO_2/SS	1.6×10^{-9}	0.94	7.20×10^{7}
E-SiO_2-LO/SS	1.4×10^{-9}	0.96	1.95×10^{8}

[a] Epoxy resin

3.3.3.2. Investigation of non-defected coatings in different immersion times

Impedance studies were performed on the non-defected coatings after various immersion times to estimate the anticorrosive characteristics and the effect of the SiO_2 microstructures as well as the presence of LO on the coatings at the various immersion times. Fig 11 shows the variations of the $|Z_{10\ mHz}|$ at various immersion periods. The electrolyte could diffuse into the interfacial area of the coating material and steel surface. Following electrolyte diffusion, the electrochemical reactions that are responsible for the corrosion of steel surfaces can be started [52]. It was generally accepted that by increasing the time of immersion, the corrosion resistance was reduced correspondingly. This happens because of the diffusion of water molecules and ionic species (exist in the electrolyte) along with dissolved oxygen molecules through the coating layer into the metal surface [34]. A similar trend was observed for all samples, whereas the composite coating showed a negligible decrease in $|Z_{10\ mHz}|$ as compared to other samples. Rather than the hydrophobic benign of LO within the composition of the E-SiO_2-

LO/SS, this compound shows self-healing characteristics as reported previously [35,43]. For all coated steel panels, the impedance quantities at 10 MHz reduced with enhancing the time of immersion, which manifested that by the enhancing of immersion time, the corrosive ions, oxygen, and water molecules gradually penetrated through the coatings, resulting in a decrease of the impedance modulus. So, the composite coating containing LO showed the least decrease in $|Z_{10\ mHz}|$ as compared with the two other samples, which is related to the limited diffusion of corrosive species to the interface of metal surface-coating. This could be also further explained by the fact that the epoxy resin utilized here, is polar and so it has a significant affinity to absorb water. This water tendency could subsequently create corridors for the diffusion of corrosive species, which could finally result in the corrosion of the under layered steel substrate. Moreover, as it can be seen, the E-SiO_2/SS shows higher $|Z_{10\ mHz}|$ when compared to the pure epoxy coating steel panel. The formation of Si-O-Si binding through exposure to corrosive media may be responsible for the better anticorrosive performance of the E-SiO_2/SS [53]. It can be emphasized that for each point of presented data, three runs have been done, and the average values were reported.

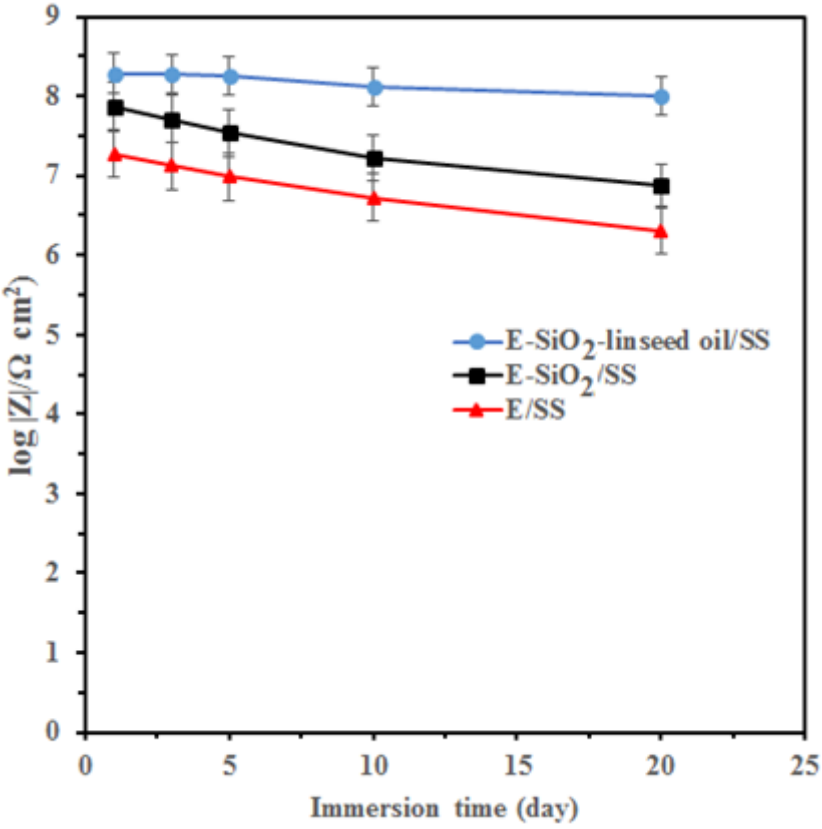

Figure 11. Log $|Z_{10\ mHz}|$ variations against immersion time for non-defected E, E-SiO_2, and E-SiO_2-LO coated steel panels

3.3.3.3. Impedance spectra for scratched samples

Creating a defect in the coated steel panels meaningfully altered the impedance modulus of the samples because of the direct contact between the metal surface and the corrosive media. The direct contact between naked metal and corrosive media triggers the metal corrosion. Fig 12 displays the typical Bode plots of the defected coated steel panels after 96 h of immersion in saline media. The impedance modulus was quite different from the impedance spectra of non-defected steel panels. Impedance spectra for scratched samples were fitted to the equivalent circuit displayed in Fig. 12C. The related fitted data of the EIS plots are presented in Table 3. In the

applied equivalent circuit, R_s, R_{ct}, CPE_{dl}, R_{coat}, and CPE_{coat} stand for the solution resistance, charge transfer resistance at the interface of the steel panel and electrolyte, non-ideal double layer capacitor related to the interface of steel support and electrolyte, coating resistance, and a non-ideal capacitor formed at the interfacial area between electrolyte and coating material, respectively.

When a defect was deduced in the self-healing coating material, the embedded healing agent should be available to release near the crack location in such a way that the least negative effect on the barrier performance was visible. Thus, it can be revealed from the results that the composite coating containing both LO and SiO_2 microspheres played superior barrier performance in the epoxy coating, even after creating a defect on the surface of epoxy composite coated steel panel. When the results were compared to the non-defected samples, it could be clearly understood that the created defect also deteriorates the integrity of both coatings including neat epoxy and E-SiO_2. Thus, the pure epoxy coating showed the highest anti-corrosion performance deterioration when compared to E-SiO_2/SS and E-SiO_2-LO/SS coated samples. It seems that the neat epoxy coating shows the highest water uptake capability among various scratched coatings owing to its highest value of coating capacitance (Table 3). Another issue that could be pointed out from Fig 12B is that the time constant of the E-SiO_2 is located in a lower frequency region (this quantity manifests that the corrosion process happens at the interfacial area between the steel support and the electrolyte, which could be principally ascribed to the double-layer capacitor) as compared to the neat epoxy coating steel panel revealing the block effect of SiO_2 [15]. The lowest $|Z_{10\ mHz}|$ among the coated steel panels manifests the lowest anticorrosion performance of the pure epoxy coating material. As mentioned previously, the higher the coating capacitance, the higher the water uptake and lower anticorrosion performance (Table 3). The self-healing action of LO can protect the steel surface from corrosion for a nearly long period (time of this study, 96 h) as evidenced by small changes in the R_{coat} of the steel coated composite sample before and after the creation of a defect (the R_{coat} value was decreased from 8.21×10^7 to $8.4\times10^5\ \Omega\ cm^2$). Moreover, the $|Z_{10\ mHz}|$ of the defected composite coating during exposure to NaCl corrosive media did not change significantly, which is in line with a R_{coat} trend (1.92×10^8 to $1.05\times10^8\ \Omega\ cm^2$). The healing act is supplemented by blocking the coating's pores by LO as a healing agent. It seems that an adequate amount of healing agent is available in the defective area, which attains high self-healing performance. The results of EIS confirm the synergistic effect between the silica particles and LO which strengthens the anticorrosion characteristics of the composite coating containing epoxy resin when compared to pure epoxy coating steel substrate. On the other hand, the simultaneous introduction of silica microspheres and LO by simple electrodeposition method has a great effect on slowing down the corrosion of under layered steel substrate.

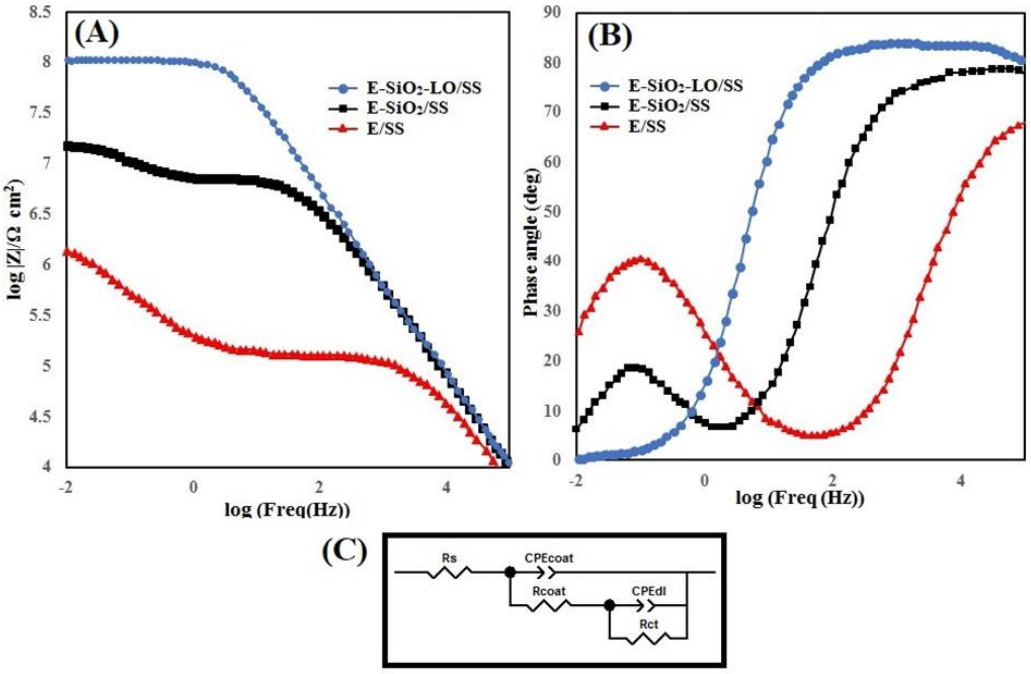

Figure 12. Typical Bode (A) and phase angle (B) plots of defected E/SS, E-SiO_2/SS, and E-SiO_2-LO/SS after immersion in 3.5 wt% NaCl solution for 96 h, (C) Electrical equivalent circuit utilized for modeling of impedance spectra

Table 3. The electrochemical parameters of scratched coated steel samples including E/SS, E-SiO_2/SS, and E-SiO_2-LO/SS after immersion in 3.5 wt% NaCl solution for 96 h

Electrode	CPE_{coat}		R_{coat} (Ω cm^2)	CPE_{dl}		Rct (Ω cm^2)
	Y_0 (Ω^{-1} $cm^{-2}S^n$)	n_{coat}		Y_0 (Ω^{-1} $cm^{-2}S^n$)	n_{dl}	
E/SS	5×10^{-6}	0.79	8.4×10^5	6.6×10^{-9}	0.81	5.2×10^5
E-SiO_2/SS	2×10^{-9}	0.92	1.5×10^6	5.6×10^{-9}	0.79	1.1×10^6
E-SiO_2-LO/SS	1.5×10^{-9}	0.94	8.21×10^7	-	-	ND*

* Negligible decrease

3.3.3.4. Investigation of non-defected coatings in different immersion times

The variation in impedance modulus at 10 MHz against the immersion time for the various steel coated samples is given in Fig 13. By increasing the immersion time (i.e., 96 h), the $|Z_{10\ mHz}|$ value is further remarkably reduced for neat epoxy coating steel panels. The $|Z_{10\ mHz}|$ value for the composite epoxy coating remains nearly the same during the immersion in NaCl media for a nearly long period, whereas those of the E-SiO_2/SS and E/SS coatings start to decrease owing to the diffusion of corrosive ions following the defect formation. This confirms that the anticorrosive performance of a composite coating is much better than that of E-SiO_2/SS and E/SS coatings, which is ascribed to the involvement of a self-healing component (LO) in the corrosion process. The superior self-healing performance of the composite coating may be ascribed to the formation of the compact film as evidenced also by the SEM image (Fig. 2). The higher $|Z_{10\ mHz}|$ values for E-SiO_2/SS in comparison with E/SS in all the immersion times were also related to the presence of silica particles and condensation of these particles following the diffusion of water after creation of an artificial crack. Thus, based on the EIS studies, it can be concluded that the self-healing composite epoxy coating can preserve the corrosion resistance performance even after defect formation.

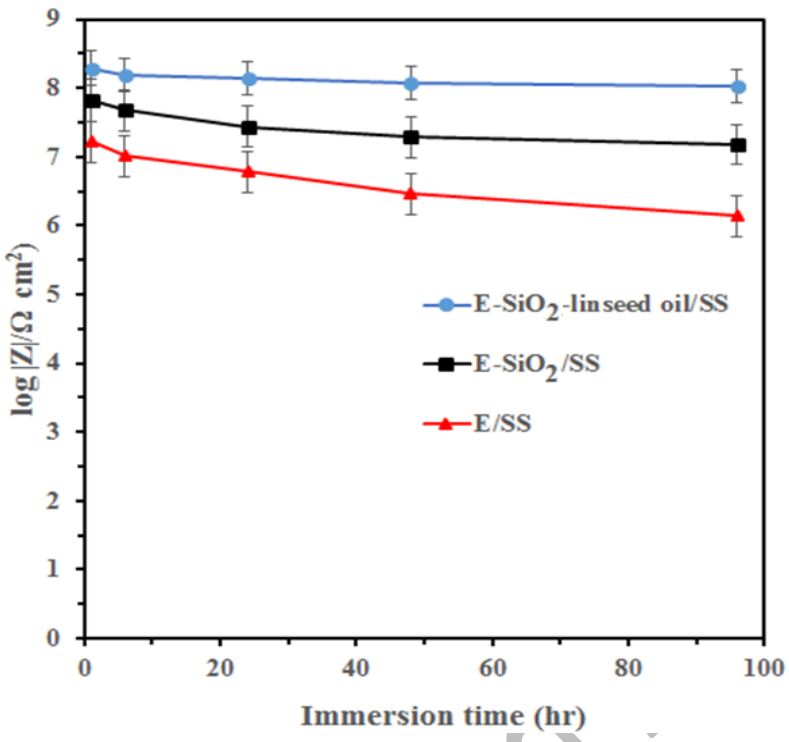

Figure 13. Log $|Z_{10\ mHz}|$ variations against immersion time for scratched E, E-SiO_2, and E-SiO_2-LO coated steel panels.

3.4. Salt spray

The salt spray test, also known as the salt fog test or salt corrosion test, is a common method used to evaluate the corrosion resistance of materials and coatings. It simulates the effects of salt-laden environments, such as coastal or marine atmospheres, on the tested samples.

The salt spray test was conducted to assess the anticorrosion performance of the self-healing coatings. Typically, the salt spray test follows a standardized procedure outlined by international standards such as ASTM B117 or ISO 9227. Here is a general overview of the salt spray test procedure:

1- Test Chamber: The test is performed in a salt spray test chamber, which provides a controlled environment for the exposure of the samples to a salt fog.

2- Sample Preparation: The coated steel samples, in this case, the self-healing coatings based on epoxy resin decorated with SiO_2/LO, would have been prepared and mounted in the test chamber.

3- Salt Solution Preparation: A salt solution is prepared by dissolving salt, typically sodium chloride (NaCl), in distilled water to create a solution with a specific concentration.

4- Test Conditions: The test chamber is set to maintain specific conditions, including temperature, humidity, and duration of exposure.

5- Salt Spray Exposure: The salt solution is sprayed as a fog or mist into the test chamber, creating a corrosive environment. The samples are exposed to this salt fog for a predetermined period, which can range from hours to hundreds of hours, depending on the testing requirements.

6- Evaluation: After the exposure period, the samples are removed from the test chamber, cleaned, and evaluated for signs of corrosion. Various techniques and analyses can be used to assess corrosion resistance, such as visual inspection, measurement of corrosion products, weight loss determination, or surface characterization using microscopy or spectroscopy techniques.

The salt spray test was implemented on the scratched pure epoxy, epoxy/SiO_2, and epoxy-LO-SiO_2 coatings after 96 h, and the digital photos of the coatings are given in Fig 14. In the case of neat epoxy coating (Fig. 13A), several numbers of blisters and rusty areas were observed near the defects, demonstrating the low anticorrosion efficiency of pure epoxy coating after scratch formation. This finding specifies that the corrosive ions and oxygen could simply penetrate the defects and the reactions of these species corrode the surface of the steel panel. Thus, for E-SiO_2/SS (Fig 14B), although there are still some blisters and rusty spots, it seems that the corrosion rate of this coating is slower than that of a pure epoxy coating steel panel. Results demonstrate that the epoxy coating loaded with both electrochemically precipitated SiO_2 and LO displays good anti-corrosion/self-healing performance. The composite coating represents a negligible blistering zone, as clearly shown in Fig 14C. This observation could be ascribed to the presence of a film of LO on the metal surface. The salt spray test studies specify that the use of LO in line with silica microparticles in the epoxy coating significantly increased its anti-corrosion/self-healing activity.

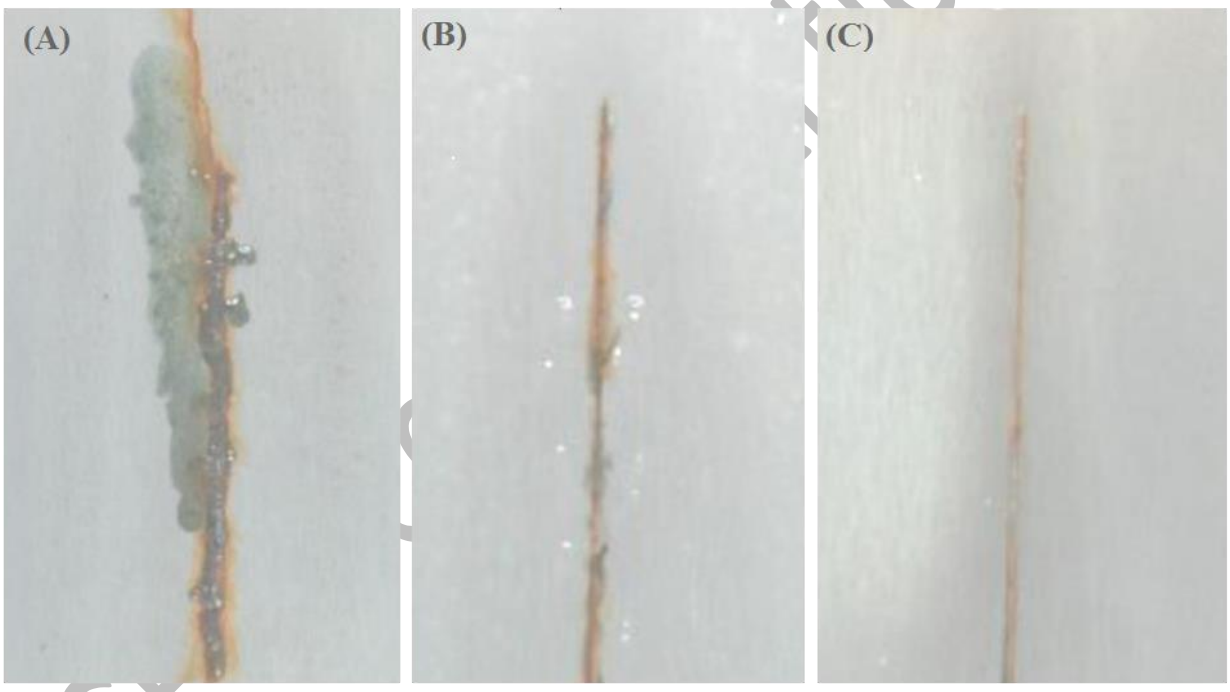

Figure 14. Digital photos of coated steel panels during exposure to salt spray test after 96 h, (A) E/SS, (B) E-SiO_2/SS, and, (C) E-SiO_2-LO/SS

3.5. Mechanism of cathodic reactions in anticorrosion process

Corrosion of coated metallic supports takes place in three stages, including water absorption on the coating, transportation of corrosive reagents into the coating, and reaching of these reagents to the coating/metal interfacial area. When corrosive reagents touch the metal surface, a corrosion reaction starts and several oxidation and reduction reactions which are responsible for the corrosion process happen. In the anodic branch of corrosion, iron is oxidized and Fe (II) and Fe (III) ions are released from the steel substrate. On the contrary, in the cathodic branch, O_2 is reduced by released electrons from the anode through an external circuit. However, the coatings could slow down the corrosion process by retarding the redox reactions (Scheme 2). The LO can form a solid and compact film after the creation of a scratch, as witnessed by SEM images of the electrochemically deposited silica

microspheres/LO (Figs. 2D, 2E, and 2F). This is because the fact that the LO comprises a significant quantity of unsaturated fatty acids, which contain carbon–carbon double bonds and could be easily oxidized by oxygen and form a film on the surface of defected epoxy coating steel [35]. Finally, the film formation significantly retards the corrosion of the under layered steel surface. A comparison of optical images affirms that the crack was healed by the loading of LO within the composition of the composite coating. As noticed above, the pure epoxy coating exhibited poor anti-corrosion performance after creating a crack on the surface of the pure epoxy coated steel panel. When the corrosion procedure happens, the defects can act as diffusion pathways for corrosive species such as Cl^-, O_2, and H_2O. It seems that silica microspheres could not completely block the diffusion pathways related to corrosive species, and there are still some pathways for ions and corrosive species diffusion. The addition of LO to the electrodeposition media results in increasing the barrier performance of the composite coating as witnessed by EIS studies (Fig 8). Thus, after epoxy painting of SiO_2-LO coated steel, fewer penetration pathways are available for diffusion of corrosive media to the steel support.

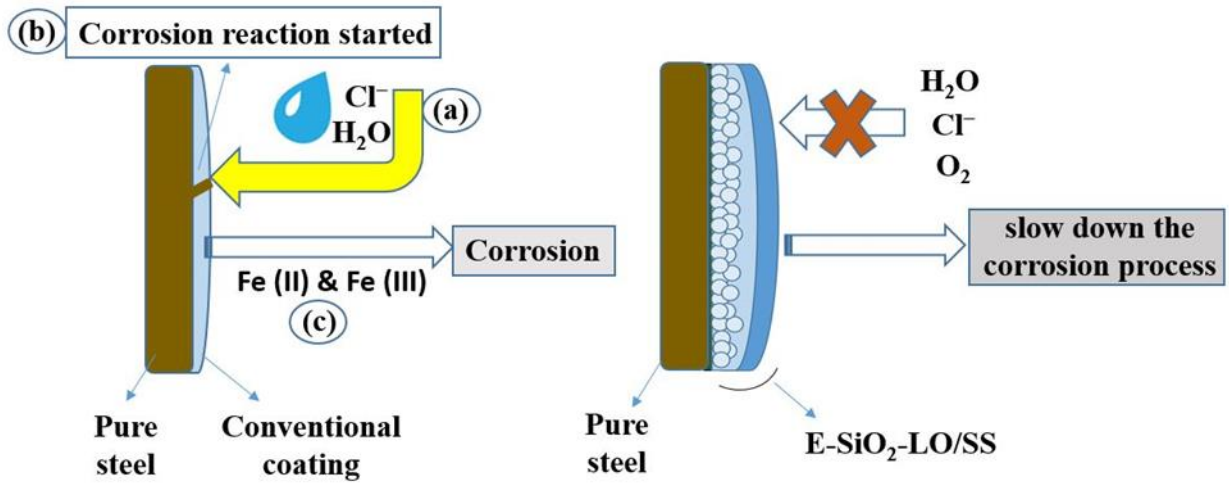

Scheme 2. Mechanism of cathodic reactions in anticorrosion property by synthesized coating

3.6. Comparative study

The protection performance of the coated mild steel sample was compared with other similar researches in the literature and the results were displayed in Table 4. These findings further dedicate the outstanding anticorrosion performance of the E/SiO_2-LO coating layer on mild steel support.

Table 4. Literature survey of Anticorrosion performance comparison of epoxy coated electrodeposited SiO2-linseed oil

Sample	E_{corr} (mV)	I_{corr} (μA/cm^2)	R_{ct}(Ω cm^2)	Reference
E/SiO_2-LO	*-473*	0.091	1.95×10^8	This work
MGel/GO-EP[a]	-267	0.068	5.046×10^7	[54]
MGel/EP[b]	-416	0.4565	9.080×10^6	[54]
PPY/GO-EP[c]	-562	0.0018	5.142×10^6	[55]
GO-PCL[d]	-394	0.01	1.784×10^8	[56]
TGETET/DAH[e]	-617.5	0.89	2170	[57]
TGETET/DDM[f]	-557.6	0.73	3794	[57]
SF-MKPC (BP-4)	-334.13	0.0242	2.25×10^6	[58]

[a]Modified gelatin/graphene oxide/epoxy, [b]Modified gelatin/epoxy, [c] polypyrrole/graphene oxide-epoxy, [d] graphene oxide-polycaprolactone, [e]Triglycidyl ether triethoxy triazine (TGETET) epoxy resin cured by 1.6-diaminohexane, [f] Triglycidyl ether triethoxy triazine epoxy resin cured by 4.4-diaminodiphenyl methane, [g] silica fume coated magnesium potassium phosphate cement.

4. Conclusion

In this work, one-step electrochemical deposition as a facile and rapid route was utilized for the precipitation of SiO_2/LO on the surface of the steel substrate. Characterization of electrodeposited SiO_2 and SiO_2/LO was surveyed using FTIR, SEM, EDX, TGA, and XRD. SEM images revealed that the silica particles were spherical in morphology and after introducing LO to the electrodeposition bath, a compact film of LO was formed within and on the surface of SiO_2 microspheres. The electrodeposited SiO_2/LO in combination with epoxy resin created a coating with better healing and corrosion protection properties. The lower decline in impedance modulus at low frequency and also larger R_{coat} of composite epoxy coating are signs of better anticorrosion performance of the composite coating. The superior self-healing ability of E-SiO_2-LO/SS composite coating is also confirmed by impedance studies on injured coatings submerged in saline media. More interestingly, optical images of scratched samples revealed the self-healing ability of the composite coating. The protective mechanism of the composite coating containing LO and SiO_2 microspheres was ascribed to the synergistic effect between the components and the self-healing capability of LO, that could impede against the invasion of corrosive species into the metal substrate.

Acknowledgements

The authors gratefully thankful of financial support from Islamic Azad University of Tehran, Science and Research Branch.

Conflict of interest

The authors declare that they have no conflict of interest.

References:

[1] Habibiyan, A., Ramezanzadeh, B., Mahdavian, M., Bahlakeh, G., Kasaeian, M., Rational assembly of mussel-inspired polydopamine (PDA)-Zn (II) complex nanospheres on graphene oxide framework tailored for robust self-healing anti-corrosion coatings application. Chem. Eng. J. **391**: 123630, (2019).

[2] Sambyal, P., Ruhi, G., Dhawan, S., Bisht, B., Gairola, S. Enhanced anticorrosive properties of tailored poly (aniline-anisidine)/chitosan/SiO2 composite for protection of mild steel in aggressive marine conditions. Prog. Org. Coat. **119**: 203-213, (2018).

[3] Twite, R., Bierwagen, G. P. Review of alternatives to chromate for corrosion protection of aluminum aerospace alloys. Prog. org. coat. **33**: 91-100 (1998).

[4] Gharbi, O., Thomas, S., Smith, C., Birbilis, N., Chromate replacement: what does the future hold? NPJ Mater. Degrad. **2**: 1-8 (2018).

[5] Cao, Y., Chen, C., Lu, X., Xu, D., Huang, J., Xin, Z., Bio-based polybenzoxazine superhydrophobic coating with active corrosion resistance for carbon steel protection. Surf. Coat. Technol. **405**: 126569, (2021).

[6] Liu, Y.H., Xu, J.B., Zhang, J.T., Hu, J.M., Electrodeposited silica film interlayer for active corrosion protection. Corros. Sci. **120**: 61-74, (2017).

[7] Arabzadeh, H., Shahidi, M., Foroughi, M.M., Electrodeposited polypyrrole coatings on mild steel: Modeling the EIS data with a new equivalent circuit and the influence of scan rate and cycle number on the corrosion protection. J. Electroanal. Chem. **807**: 162-173, (2017).

[8] Abd El-Lateef, H. M., Khalaf, M.M., Fabrication and characterization of alumina-silica/poly (o-toluidine) nanocomposites as novel anticorrosive epoxy coatings films on carbon steel. Microchem. J. **158**: 105129, (2020).

[9] Zhang, T., Liu, W., Dong, B., Mao, R., Sun, Y., Chen, L., Corrosion of Cu-doped Ni–Mo low-alloy steel in a severe marine environment. J. Phys. Chem. Solids **163**: 110584, (2022).

[10] Jafari, H., Danaee, I., Eskandari, H., RashvandAvei, M., Combined Computational and Experimental Study on the Adsorption and Inhibition Effects of N2O2 Schiff Base on the Corrosion of API 5L Grade B Steel in 1 mol/L HCl, Journal of Materials Science & Technology. **30**: 239-252, (2014).

[11] Jafari, H., Danaee, I. Eskandari, H., RashvandAvei, M., Electrochemical and Theoretical Studies of Adsorption and Corrosion Inhibition of N,N′-Bis(2-hydroxyethoxyacetophenone)-2,2-dimethyl1,2-propanediimine on Low Carbon Steel (API 5L Grade B) in Acidic Solution, Ind. Eng. Chem. Res. **52**: 6617–6632,(2013).

[12] Jafari, H., Akbarzade, K., Danaee, I., Corrosion inhibition of carbon steel immersed in a 1 M HCl solution using benzothiazole derivatives, Arabian Journal of Chemistry. **12**: 1387-1394, (2019).

[13] Jafari, H., Ameri, E., Rezaeivala, M., Berisha, A., Halili, J., Anti-corrosion behavior of two N_2O_4 Schiff-base ligands: Experimental and theoretical studies, Journal of Physics and Chemistry of Solids. **164**: 110645, (2022).

[14] Mobin, M., Parveen, M., Aslam, R. Effect of different additives, temperature, and immersion time on the inhibition behavior of L-valine for mild steel corrosion in 5% HCl solution. J. Phys. Chem. Solids. **161**: 110422, (2022).

[15] Shen, Y., Li, K., Chen, H., Wu, Z., Wang, Z., Superhydrophobic F-SiO2@ PDMS composite coatings prepared by a two-step spraying method for the interface erosion mechanism and anti-corrosive applications. Chem. Eng. J. **413**: 127455, (2021).

[16] Zhang, F., Ju, P., Pan, M., Zhang, D., Huang, Y., Li, G., Li, X., Self-healing mechanisms in smart protective coatings: a review. Corros. Sci. **144**: 74-88, (2018).

[17] Cui, J., Li, X., Pei, Z., Pei, Y. A long-term stable and environmental friendly self-healing coating with polyaniline/sodium alginate microcapsule structure for corrosion protection of water-delivery pipelines. Chem. Eng. J. **358**: 379-388, (2019).

[18] Ataei, S., Khorasani, S.N., Neisiany, R.E., Biofriendly vegetable oil healing agents used for developing self-healing coatings: A review. Prog. Org. Coat. **129**: 77-95 (2019).

[19] Song, Y., Chen, K.F., Wang, J.J., Liu, Y., Qi, T., Li, G.L., Synthesis of polyurethane/poly (urea-formaldehyde) double-shelled microcapsules for self-healing anticorrosion coatings. Chinese J. Polym. Sci. **38**: 45-52, (2020).

[20] Wang, Z., Scheres, L., Xia, H., Zuilhof, H., Developments and Challenges in Self-Healing Antifouling Materials. Adv. Funct. Mater. **30**: 1908098, (2020).

[21] Nazeer, A. A., Madkour, M., Potential use of smart coatings for corrosion protection of metals and alloys: A review. J. Mol. Liq. **253**: 11-22, (2018).

[22] Li, K., Li, H., Cui, Y., Li, Z., Ji, J., Feng, Y., Chen, S., Zhang, M., Wang, H. Dual-functional coatings with self-lubricating and self-healing properties by combining poly (urea–formaldehyde)/SiO2 hybrid microcapsules containing linseed oil. Indust. Eng. Chem. Res. **58**: 22032-22039, (2019).

[23] Lu, T., Li, B., Sun, D., Hu, M., Ma, J., Sun, G. Advances in controlled release of microcapsules and promising applications in self-healing of asphalt materials. J. Clean. Prod. 126270 (2021).

[24] Shchukina, E., Wang, H., Shchukin, D.G., Nanocontainer-based self-healing coatings: current progress and future perspectives. ChemComm. **55**: 3859-3867, (2019).

[25] Dezfuli, S. M., Sabzi, M. Deposition of self-healing thin films by the sol–gel method: a review of layer-deposition mechanisms and activation of self-healing mechanisms. Appl. Phys A. **125**: 1-8, (2019).

[26] Sun, H., Hammann, B. A., Brady, A. B., Singh, G., Housel, L. M., Takeuchi, E. S., Takeuchi, K. J., Marschilok, A. C., Hayes, S. E., Szczepura, L. F. Structural Investigation of Silver Vanadium Phosphorus Oxide (Ag2VO2PO4) and Its Reduction Products. Chem. Mater. **33**: 4425-4434, (2021).

[27] Brownt, E.N., Kessler, M.R., Sottost, N.R., Whites, S.R., In situ poly(urea-formaldehyde) microencapsulation of dic yclopentadiene, Journal of Microencapsulation. **20**: 719-730, (2003).

[28] Nesterova, T., Dam-Johansen, K., Thorslund Pedersen, L., Kiil, S., Microcapsule-based self-healing anticorrosive coatings: Capsule size, coating formulation, and exposure testing, Prog. Org. Coat. **75**: 309–318, (2012).

[29] Swamy, N.K., Mohana, K.N.S., Hegde, M.B., Madhusudana, A.M., Fabrication of 1D graphene nanoribbon and malenized linseed oil-based nanocomposite: a highly impervious bio-based anti-corrosion coating material for mild steel. J. Appl. Electrochem. **52**: 1133–1148, (2022).

[30] Shahabudin, N., Yahya, R., Neon Gan, S., Microencapsulation of a Palm Oil-based Alkyd by Amino Resins, Macromol. Symp. **354**: 305–313, (2015).

[31] Kongparakul, S., Kornprasert, S., Suriya, P., Lea, D., Samart, C., Chantarasiri, N., Prasassarakich, P., Guan G., Self-healing hybrid nanocomposite anticorrosive coating fromepoxy/modified nanosilica/perfluorooctyl triethoxysilane, Prog. Org. Coat. **104**: 173–179, (2017).

[32] Attaei, M., Calado, L.M., Taryba, M.G., Morozov, Y., R., Abdul Shakoor, Kahramand, R., Marques, A.C., Fátima Montemor, M., Autonomous self-healing in epoxy coatings provided by high efficiency isophorone diisocyanate (IPDI) microcapsules for protection of carbon steel, Prog. Org. Coat. **139**: 105445, (2020).

[33] Shisode, P.S., Patil, C.B., Mahulikar, P.P. Preparation and characterization of microcapsules containing soybean oil and their application in self-healing anticorrosive coatings. Polym Plast Technol. Eng. **57**: 1334-1343, (2018).

[34] Hasanzadeh, M., Shahidi, M., Kazemipour, M., Application of EIS and EN techniques to investigate the self-healing ability of coatings based on microcapsules filled with linseed oil and CeO_2 nanoparticles. Prog. Org. Coat. **80**: 106-119, (2015).

[35] Lang, S., Zhou, Q., Synthesis and characterization of poly (urea-formaldehyde) microcapsules containing linseed oil for self-healing coating development. Prog. Org. Coat. **105**: 99-110, (2017).

[36] Li, H., Cui, Y., Li, Z., Zhu, Y., Wang, H., Fabrication of microcapsules containing dual-functional tung oil and properties suitable for self-healing and self-lubricating coatings. Prog. Org. Coat. **115**: 164-171, (2018).

[37] Tiringer, U., Durán, A., Castro, Y., Milošev, I., Self-healing effect of hybrid sol-gel coatings based on gptms, teos, SiO_2 nanoparticles and ce (no3) 3 applied on aluminum alloy 7075-t6. J. electrochem. soc. **165**: C213, (2018).

[38] Wu, X.F., Zholobko, O., Zhou, Z., Rahman, A., Electrospun nanofibers for interfacial toughening and damage self-healing of polymer composites and surface coatings. Electrospun Polymers and Composites. Elsevier. 315-359, (2021).

[39] Shahrokhian, S., Mohammadi, R., Amini, M.K., In–situ electrochemical exfoliation of Highly Oriented Pyrolytic Graphite as a new substrate for electrodeposition of flower like nickel hydroxide: application as a new high–performance supercapacitor. Electrochim. Acta. **206**: 317-327, (2016).

[40] Ziyatdinova, G., Budnikov, H. Electroanalysis of antioxidants in pharmaceutical dosage forms: state-of-the-art and perspectives. Monatsh. Chem. **146**: 741-753, (2015).

[41] Wu, L.K., Hu, J.M., Zhang, J.Q. One step sol–gel electrochemistry for the fabrication of superhydrophobic surfaces. J. Mater. Chem. A. **1**: 14471-14475, (2013).

[42] Zhang, X.-F., Chen, Y.Q., Hu, J.M. Robust superhydrophobic SiO2/polydimethylsiloxane films coated on mild steel for corrosion protection. Corros. Sci. **166**: 108452, (2020).

[43] Behzadnasab, M., Mirabedini, S., Esfandeh, M., Farnood, R., Evaluation of corrosion performance of a self-healing epoxy-based coating containing linseed oil-filled microcapsules via electrochemical impedance spectroscopy. Prog. Org. Coat. **105**: 212-224, (2017).

[44] Szabó, T., Telegdi, J., Nyikos, L., Linseed oil-filled microcapsules containing drier and corrosion inhibitor–Their effects on self-healing capability of paints. Prog. Org. Coat. **84**, 136-142, (2015).

[45] Zhou, F., Ma, Y., Chen, Y., Zhang, L., Sheng, X., Triple-function smart anticorrosion composite coating based on graphene and ZIF-8 with excellent pH-responsive self-healing and in vitro antimicrobial properties, Progress in Organic Coatings. **186**: 108007, (2024).

[46] Ren, S., Meng, F., Li, X., Cui, Y., Liu, R., Liu, Y., Hu, X., Liu, L., Wang, F., A self-healing epoxy composite coating based on pH-responsive PCN-222 smart containers for long-term anticorrosion of aluminum alloy, Corrosion Science. **221**: 111318, (2023).

[47] Liu, Y.H., Xu, J.B., Zhang, J.T., Hu, J.M., Electrodeposited silica film interlayer for active corrosion protection, Corrosion Sci. **120**, 61-74, (2017).

[48] Ahkam, Q. M., Khan, E. U., Iqbal, J., Murtaza, A., Khan, M.T., Synthesis and characterization of cobalt-doped SiO2 nanoparticles. Physica B: Condens Matter. **572**: 161-167, (2019).

[49] Hu, C., Chen, W., Li, T., Ding, Y., Yang, H., Zhao, S., Tsiwah, E. A., Zhao, X., Xie, Y. Constructing non-fluorinated porous superhydrophobic SiO_2-based films with robust mechanical properties. Colloids Surf A: Physicochem. Eng. Asp. **551**: 65-73, (2018).

[50] Wang, J.K., Zhou, Q., Wang, J.P., Yang, S., Li, G.L. Hydrophobic self-healing polymer coatings from carboxylic acid-and fluorine-containing polymer nanocontainers. Colloids Surf A: Physicochem. Eng. Asp. **569**: 52-58, (2019).

[51] Xia, Y., Zhang, N., Zhou, Z., Chen, C., Wu, Y., Zhong, F., Lv, Y., He, Y. Incorporating SiO2 functionalized g-C_3N_4 sheets to enhance anticorrosion performance of waterborne epoxy. Prog. Org. Coat. **147**: 105768, (2020).

[52] Mohammadkhani, R., Ramezanzadeh, M., Saadatmandi, S., Ramezanzadeh, B. Designing a dual-functional epoxy composite system with self-healing/barrier anti-corrosion performance using graphene oxide nano-scale platforms decorated with zinc doped-conductive polypyrrole nanoparticles with great environmental stability and non-toxicity. Chem. Eng. J. **382**: 122819, (2020).

[53] Pourhashem, S., Vaezi, M. R., Rashidi, A., Investigating the effect of SiO_2-graphene oxide hybrid as inorganic nanofiller on corrosion protection properties of epoxy coatings. Surf. Coat. Technol. **311**: 282-294, (2017).

[54] Kamalon Rajitha, Kikkeri Narasimha Shetty Mohana, Avvadukkam Mohanan, Ambale Murthy Madhusudhan, Evaluation of anti-corrosion performance of modified gelatin-graphene oxide nanocomposite dispersed in epoxy coating on mild steel in saline media, Colloids and Surfaces A **587**: 1243, (2020).

[55] Amirazodi, K., Sharif, M., Bahrani, M., Polypyrrole doped graphene oxide reinforced epoxy nanocomposite with advanced properties for coatings of mild steel, M. J.Polym. Res. **26**: 244, (2019).

[56] Rajitha, K., Mohana, K.N., Application of modified graphene oxide–polycaprolactone nanocomposite coating for corrosion control of mild steel in saline medium, Mater. Chem. Phys. **241**: 122050, (2020).

[57] Hsissou, R., Benhiba, F., Echihi, S., Benzidia, B., Cherrouf, S., Haldhar, R., Ahmad Alvi, P., Kaya, S., Performance of curing epoxy resin as potential anticorrosive coating for carbon steel in 3.5% NaCl medium: Combining experimental and computational approaches, Chemical Physics Letters. **783**: 139081, (2021),.

[58] Wang, B., Lu, K., Han, C., Wu, Q., Study on anti-corrosion performance of silica fume modified magnesium potassium phosphate cement-based coating on steel, Case Studies in Construction Materials. **17**: e01467, (2022).